VOLUME 4, NUMBER 8, AUGUST 2004

NANO LETTERS

Cobalt-Based Superparamagnetic Nanorings

M. Marin-Almazo,[†,‡] D. Garcia-Gutierrez,[||] X. Gao,[||] J. L. Elechiguerra,[§] V. A. Kusuma,[§] W. M. Sampson,[#] M. Miki-Yoshida,[||,⊥] A. B. Dalton,[#] R. Escudero,[▼] and M. Jose-Yacaman*[,§,||]

Instituto Nacional de Investigaciones Nucleares, Carr. Méx.-Tol. Km 36.5, Ocoyoacac, Edo. de México, 52045, México, Facultad de Quimica, Universidad Autonoma del Estado de Mexico, Paseo Colon Esq. Tollocan. C.P. 50120, Toluca, Edo. de México, México, Department of Chemical Engineering, The University of Texas at Austin, 1 University Station C0400, Austin, Texas 78712-1062, The Texas Materials Institute, The University of Texas at Austin, 1 University Station C2201, Austin, Texas 78712-1063, Centro de Investigación en Materiales Avanzados, Miguel de Cervantes 120 Chihuahua, Chih. C.P. 31109, México, Nano Tech Institute, The University of Texas at Dallas, Richardson, Texas 75083, Instituto de Investigaciones en Materiales UNAM, Universidad Nacional Autónoma de México, México, D. F. A. Postal 70-360 C.P. 04510, México

Received April 9, 2004; Revised Manuscript Received June 1, 2004

ABSTRACT

Remarkable optical and magnetic properties were observed in a Co-thiol-polymer composite. The Co and the thiol ligand used to passivate the Co surface, instead of generating isolated nanoparticles, grow into nanorings with a radius around 2 nm. These structures consist of small clusters of metallic Co connected by alkylthiol chains. These small nanorings self-assemble into larger nanorings of ~10 nm, which in turn self-assemble into larger nanorings in the range of 100–1000 nm in size. We formed a composite by embedding the nanorings in a polymeric matrix. The resulting material presented interesting optical properties such as absorption and emission in the visible zone of the electromagnetic spectrum, and a strong nonlinear optical behavior. The absorption and emission are mainly due to the presence of an alkylthiol–cobalt complex; and the nonlinear optical behavior is due to the presence of the Co clusters inside the polymer matrix. These composites exhibit a superparamagnetic effect down to 250 K, and below this temperature presented features very similar to those observed in spin-glass-like systems. In the nanorings a remarkable phenomenon is that, in addition to the superparamagnetic behavior, we found that during measurements with an applied external field they act as giant aromatic macromolecules and a current circulates through them. The evidence of a current circulating through the nanorings in the presence of an external field tells us about the possibility to use these structures in the design of nanosystems. Our work opens new possibilities of using magnetic transition metals to fabricate nanostructured magnetooptical materials.

Research on nanoparticles based on magnetic transition metals has been centered on their magnetic properties, basically with the promise of applications in the fields of medicine and magnetic recording.[1−6] When the nanoparticles reach a critical size (approximately 14 nm for the case of Co) the so-called domain wall thickness becomes single domain.[7] For smaller nanoparticle sizes (around 5 nm for the case of Co), the magnetic anisotropy energy per particle becomes comparable to the thermal energy (kT). When this happens, thermal fluctuations induce random instabilities on the magnetic moment with time and the particles become

* Corresponding author email: yacaman@che.utexas.edu.
† Instituto Nacional de Investigaciones Nucleares.
‡ Universidad Autonoma del Estado de Mexico.
§ Department of Chemical Engineering, The University of Texas at Austin.
|| The Texas Materials Institute, The University of Texas at Austin.
⊥ Centro de Investigación en Materiales Avanzados.
The University of Texas at Dallas.
▼ Universidad Nacional Autónoma de México.

10.1021/nl049464b CCC: $27.50
Published on Web 07/02/2004

"superparamagnetic".[8] Despite important improvements such as the development of core−shell CoO−Co nanoparticles and other methods and techniques,[9,10] this superparamagnetic limit remains an obstacle for many possible applications of Co nanoparticles. On the other hand, optical properties of metallic nanoparticles have been a very active research field (for many centuries, as reviewed by Daniel and Astruc[11]). The vast amount of work has been concentrated mainly on noble metals, such as Au and Ag, basically. For many applications, the nanoparticles have to be inside of a dielectric matrix. These metal−dielectric composites prepared below the percolating limit should exhibit very strong nonlinearities in their optical and electronic properties.[12] One of these systems that have been widely studied is Ag nanoparticles in polymers, such as PMMA,[13] or epoxy resins. Very little is known about the possible uses of other transition metal nanoparticles, such as Co, for optical applications. One interest is that eventually they can combine magnetic and optical properties in a single material.

In the present work we study the synthesis of cobalt nanoparticles with a thiol ligand motivated by the possibility of finding new ways of increasing their superparamagnetic transition temperature. It was expected to synthesize particles with sizes between 1 and 14 nm, i.e., from the superparamagnetic limit (∼5 nm) to about the single domain region (∼14 nm). A new synthesis method was used. Samples were prepared starting with a solution of 0.7 mmol (0.1 g) of $CoCl_2$ in 150 mL of toluene with stirring. Then we add 1.5 mmol (0.3 mL) of 1-dodecanethiol [$CH_3(CH_2)_{11}-SH$, 98%] and 2.5 mmol (0.3 mL) of a solution 1.0 M of lithium triethylborohydride [$LiB(C_2H_5)_3H$]. After 5 h the final product was precipitated in cold ethanol, and the product obtained was dissolved in the minimum quantity of toluene needed and precipitated again in cold ethanol. This step is repeated two or three times in order to eliminate the excess of thiol. The final precipitate was then dried and a flaky structure was obtained. Some of the alkyl molecules dissolved in the toluene have the chance to coordinate with some of the Co^{2+} and form coordination complexes. These first coordination compounds act as the seed for self-assembly of surfactant molecules, creating preferential sulfur-rich sites for nucleation of Co atoms while the reducing agent is added. As a consequence of the size of the sites, we produced small clusters surrounded by thiol chains. The resulting material self-assembled into a self-supported flaky structure, as mentioned earlier, with a greenish color. Figure 1 presents an image of this flaky structure.

A closer examination by transmission electron microscopy (TEM) showed that intercalated fibers that assembled very much like the structure of a paper form this flaky structure. The resulting product was dissolved in toluene and mixed with a monomer (styrene) to prepare the Co−thiol−polymer composite. We used approximately 5 mL of styrene monomer, inhibited with 15−20 ppm of 4-*tert*-butyl-catechol. For this reaction, we decided not to remove the inhibitor, but it could have been done by shaking it with aqueous 4% in weight of potassium hydroxide solution under inert atmosphere, extracting the catechol into the aqueous phase. For

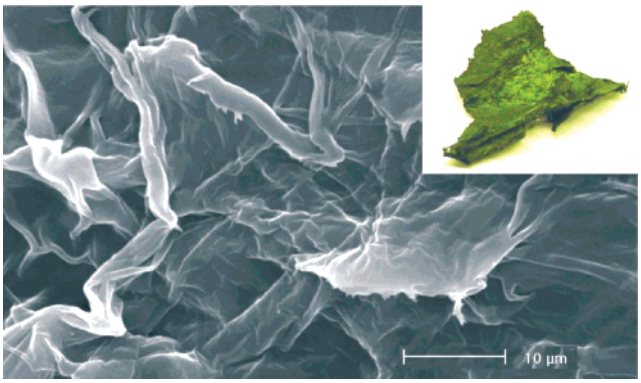

Figure 1. SEM image from the "flaky" structures obtained after purification of the final product from the nanoparticles synthesis. Inset: Photograph from the final product after removing from filtering paper.

our initiator, we weighed out either 0.1 g dicumyl peroxide or 0.1 g benzoyl peroxide. This was added into 50 mL of styrene and polymerized at room temperature over several days. The resulting composite materials were characterized by TEM, high angle annular dark field (HAADF) technique, atomic force microscopy (AFM), UV-visible absorbance, photoluminescence emission (PL), Z-scan technique experiments, and superconducting quantum interferometer device (SQUID) magnetometer measurements.

The resulting composite material showed remarkable optical properties, such as optical emission and absorption characteristics in the visible zone of the electromagnetic spectrum. We found that these properties can be modified with the concentration of Co^{2+}−thiol complexes. Figure 2 shows a few examples of different colors that can be obtained, and their corresponding UV-visible spectra. A well-defined absorption peak was found in the region near 500 nm, and the most intense emission peak was found in the region near 560 nm.

The nonlinear optical response of these composites can be measured from the normalized energy transmittance using the Z-scan method without an aperture.[14] The data can be displayed as a Z (distance) vs I (intensity) plot or direct images of the laser pulse. A laser pulse at 532 nm with a repetition rate of 1 Hz was used for this study. The pulse energy is about 150 μJ in Z-scan experiments. The spatial distribution of the pulses is nearly a Gaussian profile. The samples were placed at the focus of a lens with focal length of 30 cm for the absorptive optical limiting (OL) measurements, while they were placed at the valley position of normalized transmittance in Z-scan experiments for the refractive OL measurements. A sequence of the beam images is shown in Figure 3. In a linear optical material, changes in the position of the sample with respect to the beam source do not affect the focal point of the system; but in a nonlinear optical material, the changes in position have a direct influence on the focal point. These effects are illustrated in Figure 3. For this study the sample analyzed was the sample observed in Figure 2b.

To determine the optical properties related to the presence of the Co^{2+}−thiol complexes and the properties related to the presence of the Co−thiol nanorings, we form a composite

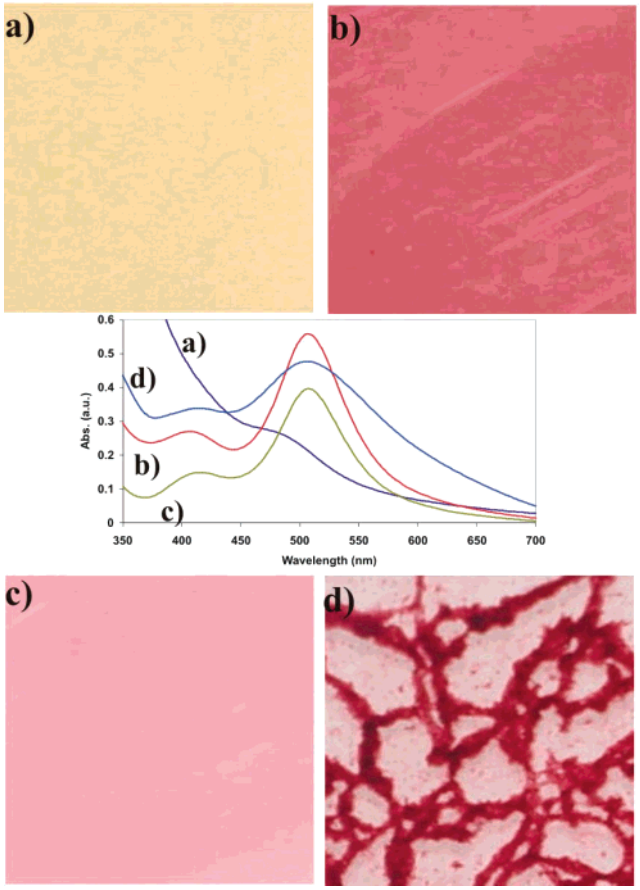

Figure 2. Image of four different composites polymer+Co^{2+}−thiol+Co systems and their corresponding UV-vis spectra. The concentration of Co and Co^{2+}−thiol was changed to produce the different absorption peaks. The polymer in (d) contains an excess of Co^{2+}−thiol.

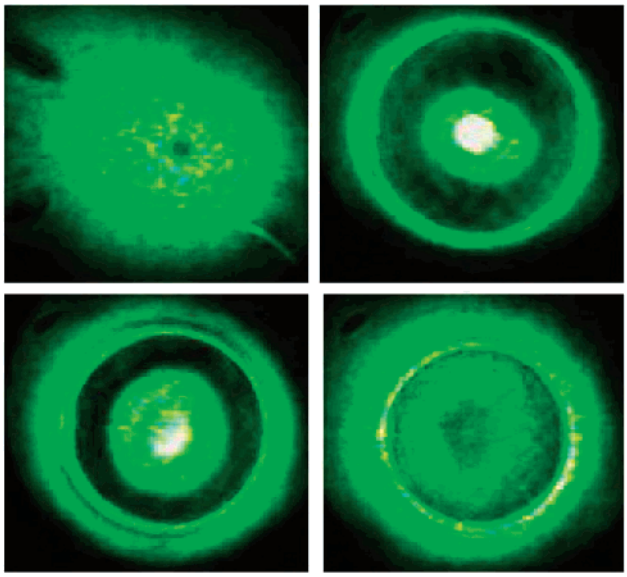

Figure 3. Sequence of beam images obtained from the Z-scan analysis. Variation in the focal point of the system illustrates the nonlinear optical behavior of the sample.

by the method described earlier; but for this composite we perform a synthesis following all the steps described above, but we did not add the reducing agent to the solution of

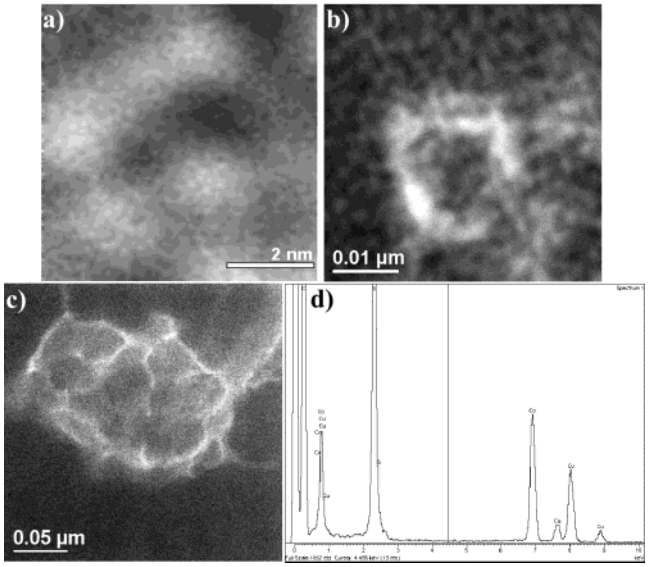

Figure 4. TEM−HAADF images of a 2 nm ring structure in a Co−thiol sample where the arrangement of the clusters can be observed. (b) A larger nanoring of 10 nm formed by units smaller than the ones shown in (a). (c) A larger structure of rings observed inside the polymer. (d) EDS pattern showing the presence of Co and S in the region shown in (c).

toluene, $CoCl_2$, and thiol. By doing these we ensure no metallic Co cluster formation and no optical effects related to them, and we also ensure the formation of the Co^{2+}−thiol complexes. From this experiment we concluded that the changes in the optical absorption and emission effects observed in the visible zone of the electromagnetic spectrum were due to the presence of the Co^{2+}−thiol complexes. However, as we mentioned above, changes in the absorption and emission properties of the composites were related to changes in the concentration of Co^{2+}−thiol complexes, and the concentration of these complexes is related to the concentration of Co metallic clusters. As the concentration of Co^{2+} decreases due to its chemical reduction, consequently decomposing the Co^{2+}−thiol complexes, metallic Co concentration starts to increase, leading to the formation of more Co clusters, changing the optical properties of the system, as can be observed in Figure 2.

However, as we mention previously, a remarkable discovery was that Co clusters, instead of growing into larger nanoparticles, tend to aggregate in nanorings. It was possible to resolve the nanorings by TEM. TEM images in the HAADF mode were used to study the Co-thiol rings. Selected HAADF images are shown in Figure 4. In the HAADF images the intensity varies, mainly, as $\sim Z^2$, where Z is the atomic number. In our case, Co becomes brighter than the carbon (polymer) background, so the nanoring configuration is very clear. A typical diameter of the rings is around 2.0 nm (Figure 4a). We found that this unit self-assembled in larger closed nanorings, as shown in Figure 4b, with a diameter of ~10 nm. Those rings grow and self-assemble in even larger structures (Figure 4c). Energy dispersive spectroscopy (EDS) analysis from this region confirms the presence of Co and S in the nanorings (Figure 4d).

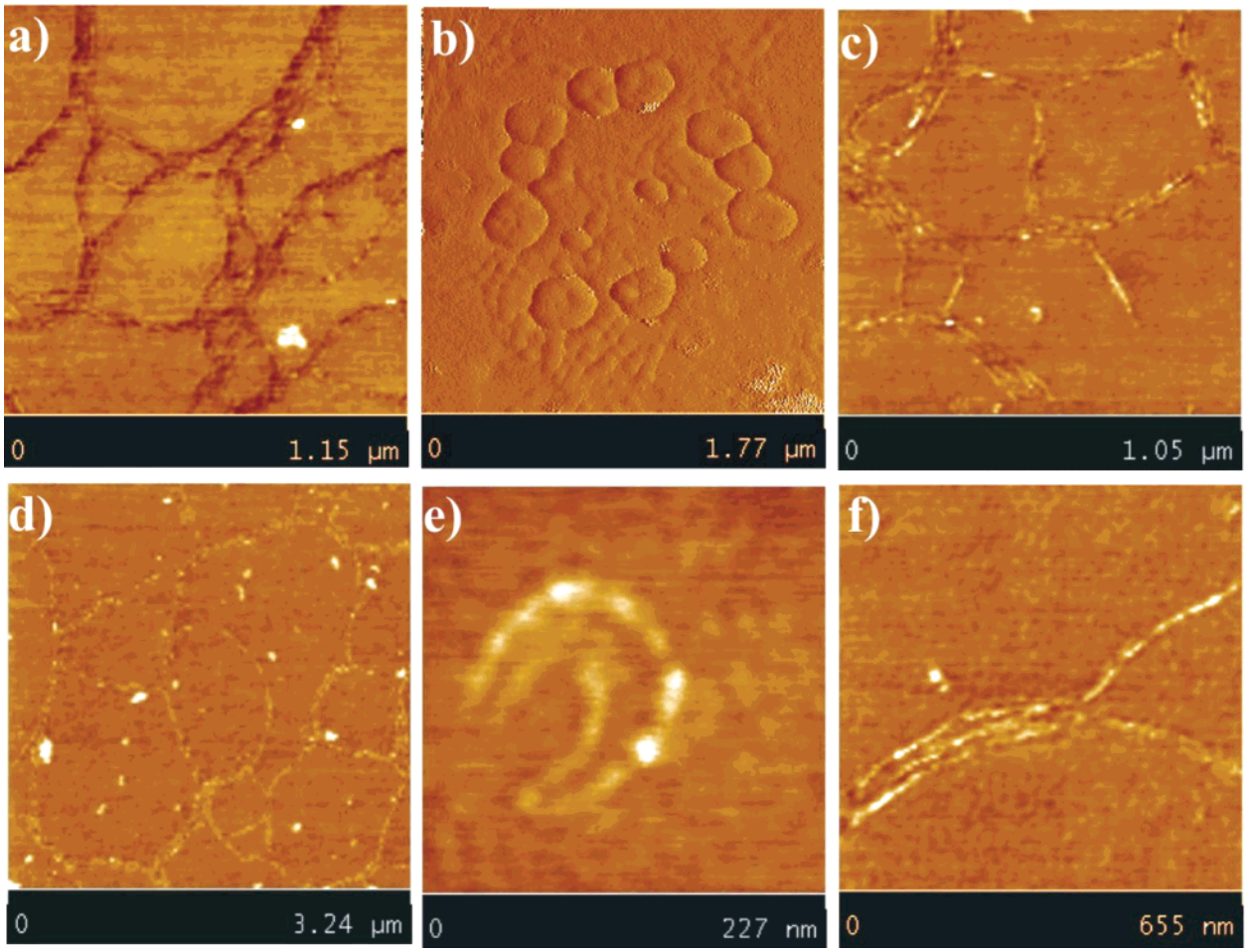

Figure 5. AFM images of different polymer composite systems. (a) Image from the sample shown in Figure 2c. (b) Image from the yellow sample shown in image 2a. (c, d, e, f) Images from a sample synthesized with the same conditions as the red one shown in Figure 2b.

Figure 5 shows examples of AFM images of different rings and other structures at the microscopic level. The images show that the rings self-assemble in larger structures. It was possible to establish a correlation between a strong absorption peak and the observed pattern. For instance, the absorption peak at 507 nm (Figure 2b) corresponds to the nanoring pattern in Figure 5c, while the pattern in Figure 5b corresponds to the peak at 470 nm (yellow film in Figure 2a). This fact illustrates the tailoring of the material optical properties at the nanometer level.

Raman spectroscopy was also performed on the Co−thiol samples, and the results are shown in Figure 6. The on-resonance and off-resonance spectra are shown in Figure 6c and 6d, respectively. Features in the on-resonance spectrum are hidden by sample luminescence, while the off-resonance spectrum confirms the presence of Co^{2+} and the alkyl character of the sample.[15] This is proof of the presence of cobalt as a divalent coordinated cation. Since we cannot resolve distinct nanoparticles in high resolution transmission electron microscopy (HRTEM), but only with the HAADF analysis, we could conclude that metallic particles are in the form of clusters with a size ≤ 1 nm; because of this size they do not produce diffraction contrast. On the other hand, some of the cobalt is coordinated to the alkyl thiols in the form of Co^{2+}. This coordination is probably octahedral. Schematic models of these structures are shown in Figure 6a and 6b.

Magnetic response of the samples was measured with a SQUID magnetometer. The field cooling (FC) and zero field cooling (ZFC) modes were used to extract the magnetization measurements. Field cooling mode consists of applying the field far above a characteristic temperature, T_B, and cooling the sample in a field to $T \ll T_B$, while recording the magnetization. Zero field cooling consists of cooling the sample in zero field to $T \ll T_B$; at this low temperature a magnetic field is applied. Then magnetic data is obtained by raising the temperature to $T \gg T_B$, keeping constant the magnetic field. The results are shown in Figure 7. In this figure we can observe magnetization vs temperature plots at two different fields. The blocking temperature, T_B, is the temperature at which superparamagnetism sets in; below this T_B the FC and ZFC curves are split.[9] From Figure 7, we can observe that T_B, for the composite observed in Figure 2b, is at about 250 K, a very high value compared with other T_B reported for very similar system of Co nanoparticles.[16−18] Skumryev et al.[9] have reported blocking temperatures for Co core/CoO shell nanoparticles of 4 nm in size embedded in an antiferromagnetic matrix (CoO) up to 290 K. In addition, both graphs show an increase in the magnetization in the FC and ZFC curves as the temperature decreases; and

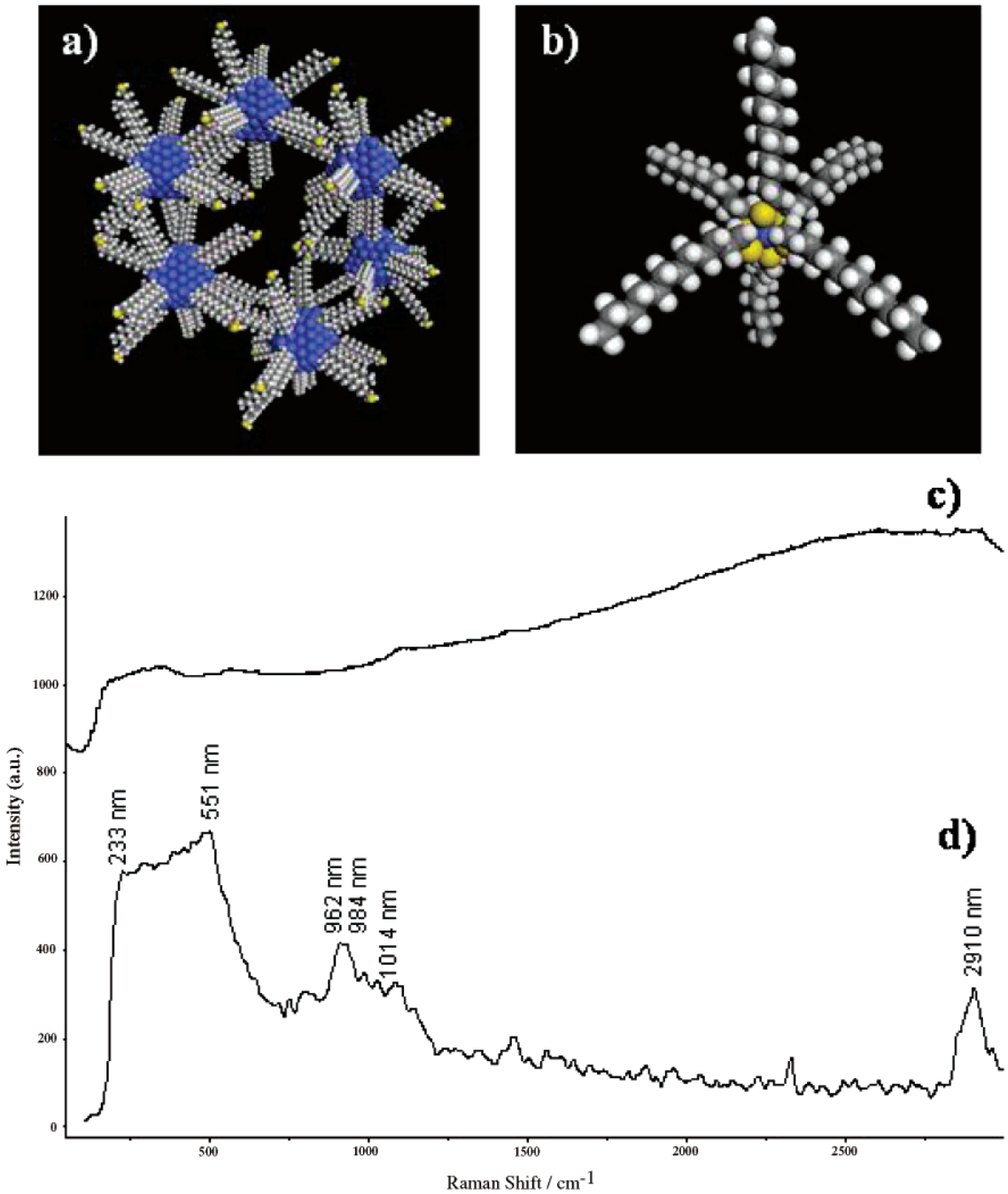

Figure 6. Schematics models and Raman spectra. (a) Schematic model showing Co−thiol-capped clusters forming a nanoring. (b) Schematic model of Co^{2+} forming an octahedral coordination complex with thiol molecules. (c) Resonance (632.8 nm) and (d) off-resonance (1064 nm) Raman spectra of the thiol-capped cobalt particles, offset for clarity. Spectral intensities are not to scale. Features in the on-resonance spectrum are hidden by sample luminescence. The feature at 2910 is attributable to the C−H stretch. Doubly ionized cobalt has low-temperature Raman features at 233, 551 (doublet), and 962, 984, 1014 (triplet),[24] which broaden and red-shift into single wide bands at room temperature, leading to the assignment of the bands between 200−500 and 900−1000 to Co^{2+}.

in the ZFC curve a maximum is observed at approximately 50 K. An increment in the FC magnetization curve with decreasing temperature and the maximum observed in the ZFC curve are characteristic features of a spin-glass-like behavior.[19] The origin of the spin-glass-like features in these kinds of systems may be explained in terms of magnetic frustrations, which originated from competing ferromagnetic and antiferromagnetic exchange interactions, deformation in the lattices, random interactions, or random distribution of magnetic ions.[19] The random distribution of the magnetic ions and deformation of the lattices are also related to the anisotropy of the system, in this case to the magnetic anisotropy, which will tend to align the spins in a preferred direction. Because of the nature of our system we believe that the anisotropy will be high; we suspect to have a lot of random interaction between the nanoparticles forming the nanorings and the Co^{2+} ions. Also, the structures in which the nanorings self-assemble, like the ones observed in Figure 5, will seem to give a random distribution of the magnetic ions, leading to a system with high anisotropy. In Figure 7

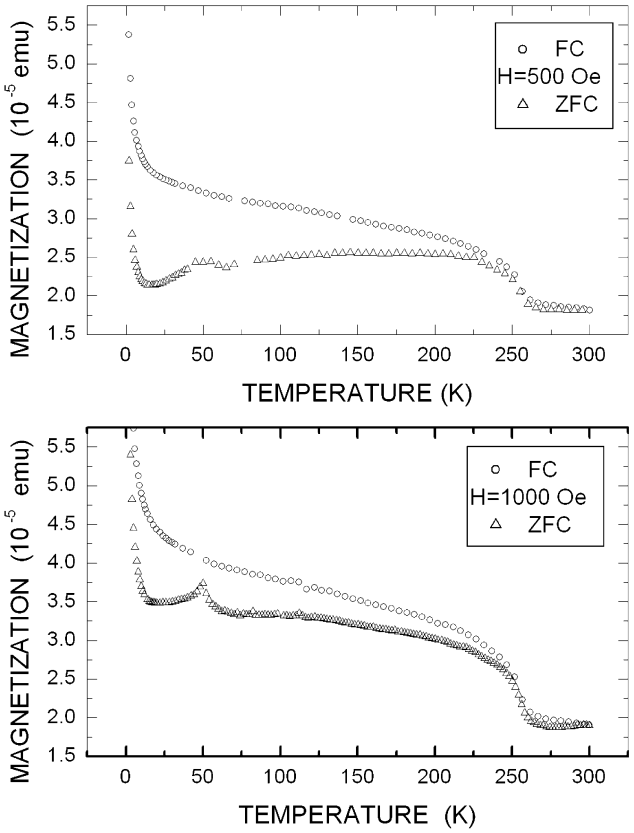

Figure 7. FC and ZFC magnetization versus temperature curves with $T_B = 250$ K for the sample observed in Figure 2b. (a) with H = 500 Oe and (b) with H = 1000 Oe.

we can also appreciate that the magnetization increases rapidly as we get closer to 0 K. We associate this increment to a second transition inside the system: a possible ferromagnetic transition. The interactions between Co nanoparticles forming the nanorings and the interactions between Co nanoparticles and Co^{2+} ions present in the Co^{2+}−thiol complexes must have an effect on the T_B as well as in the second transition observed in the magnetization vs temperatures plots.

A very interesting effect is shown in Figure 8 for the magnetization vs applied magnetic field. The hysteresis loop seems to implicate that the magnetic energy of the system under negative magnetic fields seems to be higher than the energy of the system under positive magnetic fields (area under the curve); this could be related to the anisotropy of the system. The hysteresis loop also seems to indicate that the nanorings are acting as a closed loop and a current circulates through them. This current is generated when an external field is applied to them to "screen" this external field. This phenomenon is also observed in aromatic systems. This generated current that opposes the external field will give rise to a negative contribution to the magnetization, which would have to be added to the negative magnetization arising from the polymeric matrix. Thus, we will have two contributions to the negative part of the magnetization: the intrinsic diamagnetism from the polymeric matrix and the diamagnetism from the nanorings, which seems to increase as the applied external field increases, as indicated in the inset of Figure 8. Due to the complexity of all the possible

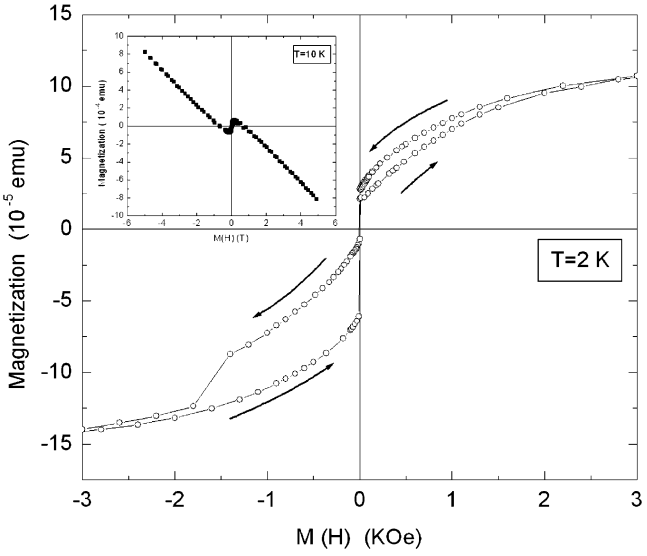

Figure 8. Magnetization vs applied magnetic field hysteresis loop at 2 K. Inset: magnetization vs applied magnetic field measured at higher field and at 10 K. Here we can observe that as the field increases, diamagnetic behavior starts to be appreciable.

interactions between all the magnetic species present in the system and their spatial arrangement, more experimental and theoretical work is required to achieve a full understanding of these interactions and their effect on the magnetic properties observed.

Puntes et al.[20] and Tripp et al.[21] have found that large magnetic Co particles can assemble in rings. For instance, Tripp has shown 27 nm Co particles forming 100 nm rings. The nanorings reported in those works are completely different phenomena since our structures are 2 orders of magnitude smaller and alkylthiol molecules bound the nanoparticles. However, the two phenomena are complementary and in both cases a magnetic flux closure is expected.

Another interesting feature of the presented ring structures is that they are produced in different length scales. The same pattern produced at a macroscopic level, visible to the bare eye (Figure 2d) also is observed in the AFM images at the microscopic level (Figure 5c), and, finally, at the nanolevel in the HAADF images (Figure 4c). Therefore, we think that the aggregation and self-assembly of the Co−thiol rings is a self-similar phenomenon and could be described by a fractal dimension.

The thiol molecules have a great influence on the growing characteristics of this system. Nanorings and other one-dimensional structures are preferred over nanoparticles. The observation of this phenomenon indicates that the energy is minimized while one-dimensional structures are formed. If we consider the nanoring in Figure 6a, a total zero magnetic moment will help to minimize the energy. Therefore, the superparamagnetic effect observed in the nanorings is to be expected. The optical emission and absorption can be explained by the presence of the Co^{2+} octahedrally coordinated to the thiols. This was proven by the results of the experiment preformed without the use of the reducing agent, described earlier in the text. The optical absorption and emission spectra for this experiment were almost identical

to those obtained for the reduced samples. In this experiment the Co^{2+} thiol complexes are produced but no nanoparticle is formed. When the reducing agent is added to the reaction and clusters ≤1 nm are formed, then strong nonlinear optical effects appear on the composite material. A metal−dielectric composite is expected to exhibit nonlinear optical properties.[12] If every nanoring is considered as a "dot", the interaction between "dots" should be considered as a dipole−dipole interaction, and $1/r^3$ dependence should be expected. Therefore, shape and aspect ratio should also play an important role in the properties observed. This material also presents superparamagnetic behavior with a blocking temperature at 250 K; below this temperature spin-glass-like features were observed, and as the temperature approached 0 K a rapid increment in the magnetization was observed, suggesting another transition, a possible ferromagnetic transition. At present, the observed effects are somehow weak, because of the small amount of Co observed in the samples, ∼1% in weight according to EDS analysis. It is clear that the newly discovered property of Co clusters to form nanorings when combining with organic ligands inside of a polymer matrix opens up the possibility of whole new applications of transition metals for magnetooptical materials.

Acknowledgment. We thank the Optics Center of the INAOE-Mexico and Dr. J. Ascencio for valuable discussions on the article. D.G. and J.E. acknowledge the support received from CONACyT Mexico.

References

(1) *Nanophotonics*, Prasad, P. N. Wiley-Interscience: New York, 2004.
(2) Bates, F. S.; Fredrickson, G. H. *Phys. Today* **1999**, *52*, 32.
(3) Thearith, U.; Liz-Marzán, L. M.; Mulvaney, P. *Colloids Surf. A* **2002**, *202*, 2−3, 119.
(4) Schuller, I. K. *Solid State Commun.* **1994**, *92*, 1−2, 141.
(5) Kodama, R. H. *J. Magn. Magn. Mater*. **1999**, *200*, 1−3, 359.
(6) Aharoni, A. *Introduction to the Theory of Magnetism*; Oxford Science Publications: Oxford, 1996.
(7) Gould. P. *Mater. Today* **2004**, February, 36.
(8) Martin, J. I.; Nogues, J.; Liu, K.; Vicent, J. L.; Schuller, I. K. *J. Magn. Magn. Mater*. **2003**, *256*, 449.
(9) Skumryev, V.; Stoyanov, S.; Zhang, Y.; Hadjipanayis, G.; Givord, D.; Nogues, J. *Nature* **2003**, *423*, 850.
(10) Puntes, V. F.; Zanchet, D.; Erdonmez, C. K.; Alivisatos, A. P. *J. Am. Chem. Soc.* **2002**, *124*(43), 12874.
(11) Daniel, M.; Astruc, D. *Chem. Rev*. **2004**, *104*, 293.
(12) Shalaev, V. M. *Phys. Rev. B* **1998**, *57*(20), 13265.
(13) Stepanov, A. L.; Popok, V. N.; Khaibulli, I. B.; Kreibig, U. *Nucl. Instrum. Methods Phys. Res. B* **2002**, *191*, 473.
(14) Qu, S.; Du, C.; Song, Y.; Wang, Y.; Gao, Y.; Liu, S.; Li, Y.; Zhu, D. *Chem. Phys. Lett.* **2002**, *356*, 403.
(15) Christie, J. H.; Lockwood, D. J. *Chem. Phys. Lett.* **1971**, *8*, 120.
(16) Osuna, J.; de Caro, D.; Amiens, C.; Chaudret, B.; Snoeck, E.; Respaud, M.; Broto, J. M.; Fert, A. *J. Phys. Chem.* **1996**, *100*, 14572.
(17) Wilcoxon, J. P.; Vneturini, E. L.; Provencio, P. *Phys. Rev. B* **2004**, *69*, 172402.
(18) Respaud, M.; Broto, J. M.; Rakoto, H.; Fert, A. R. *Phys. Rev. B* **1999**, *57*, 2925.
(19) Joy, P. A.; Anil Kumar, P. S.; Date, S. K. *J. Phys.: Condens. Matter* **1998**, *10*, 11049.
(20) Punte, V. F.; Krishnan, K. M.; Alivisatos, A. P. *Science* **2003**, *291*, 2115.
(21) Tripp, S. L.; Pusztay, S. V.; Ribbe, A. E.; Wei, A. *J. Am. Chem. Soc.* **2002**, *124*, 7914.

NL049464B